Structural Investigation of Langmuir-Blodgett Films and Tubules of 1,2-Bis(10,12-tricosadiynol)-*sn*-glycerol-3-phosphocholine ($DC_{8,9}PC$) Using Electron Diffraction Techniques

J. B. Lando* and R. V. Sudiwala

Department of Macromolecular Science, Case Western Reserve University, Cleveland, Ohio 44106

Received March 29, 1990

The phospholipid 1,2-bis(10,12-tricosadiynol)-*sn*-glycerol-3-phosphocholine ($DC_{8,9}PC$) can form open-ended hollow cylindrical structures known as tubules. To understand the mechanisms of tubule formation, we have studied the crystal structure of $DC_{8,9}PC$ in both tubules and Langmuir-Blodgett (LB) films. Using a combination of two-dimensional electron diffraction data and modeling, we find that in both cases $DC_{8,9}PC$ lies within a monoclinic unit cell of space group $P2_1$ with two molecules per unit cell. The unit cell parameters are a = 5.18 Å and b = 7.79 Å for tubules and a = 5.09 Å, b = 7.74 Å, c = 78.5 Å, and β = 117° for LB films. The b axis is the unique axis. A three-dimensional crystal structure is proposed for $DC_{8,9}PC$ within LB films.

Introduction

It has been known for some time that the polymerizable phospholipid $DC_{8,9}PC$ shown in Figure 1 can form hollow, open-ended cylindrical structures known as tubules. Yager et al.[1,2] have shown that tubules can be formed by cooling hydrated liposomes of $DC_{8,9}PC$ below its chain melt transition temperature, T_m, of 43 °C. Tubules can be formed with some degree of control over length and diameter dimensions through precipitation by the addition of water to solutions of $DC_{8,9}PC$ in a variety of alcohols at different temperatures.[3,4] In addition to tubules, open helical structures are also extensively formed by this method. Lando et al.[4,5] have shown that tubules and helices are also formed when $DC_{8,9}PC$ is precipitated from water–ethanol mixtures of fixed ratios by lowering the temperature. In this instance the temperature at which tubules are formed depends on the water–ethanol ratio, as does the final size distribution of the tubules.

The open helices formed by the last two methods have diameters and wall thicknesses the same as the tubules and may be intermediaries to tubules formation. Helfrich[20] has shown theoretically how bilayer strips of chiral molecules can form helical structures due to spontaneous torsion of the strip edges. The predicted gradient angle of the helix, 45°, agrees well with experimentally measured values of approximately 43°.[2,3,20] These helical strips then presumably widen and fuse at the edges to form the complete tubule.

An interesting feature in tubules formed by the last method is that although the overall diameter can be varied over a relatively large range by changing the water–ethanol ratio, the wall thickness remains fairly constant at 0.085 μm. We believe we have an understanding of this phenomenum based on nucleation theory, to be published later. Testing the theory requires some knowledge of the crystal structure of $DC_{8,9}PC$ not only in the tubular morphology but also in its uncurved lamellar state. Being an amphiphilic molecule, one can form flat multilayers of $DC_{8,9}PC$ using the Langmuir–Blodgett (LB) technique.[6] The crystal structures of both tubules and LB multilayers of $DC_{8,9}PC$ have been studied by using diffraction electron microscopy. We have attempted to refine the three-dimensional crystal structure of $DC_{8,9}PC$ within LB films against two-dimensional diffraction data using a combination of modeling and diffraction analysis as described in the Appendix.

Experimental Section

The $DC_{8,9}PC$ used in this work was synthesized and supplied by Yager et al. of the Bio/Molecular Engineering Branch, Naval Research Laboratory, Washington, DC. The synthesis of this material has been described elsewhere.[1,2,7,8] All preparations described below were done in a class 100 cleanroom facility equipped with class 10 work stations. The ultrapure water used in this work was produced as previously described by Shutt.[9] All glassware used was cleaned by sonication in alcoholic potassium hydroxide for 30 min (0.5 g of potassium hydroxide in 100 mL of a 50/50 spectrophotometric grade methanol/pure water mix) followed by a thorough rinse in pure water.

For electron diffraction studies LB films of six layers of $DC_{8,9}PC$ were deposited onto 200-mesh carbon-coated copper TEM grids (Polysciences, Inc., cat. no. 7289). The thinness of these films should preclude significant dynamical effects on the relative intensities of the observed reflections. A Lauda film balance with a computerized data acquisition system, previously described by Shutt,[9] was used for pressure/area isotherm collection and monolayer deposition. The $DC_{8,9}PC$ was dissolved in spectrophotometric grade chloroform to a concentration of 1 mg/mL, and 100 mL of this solution was cast onto a clean water surface to form the Langmuir film. The film was compressed at a rate of 55 cm^2/min and held at a surface pressure of 35 dyn/cm during deposition. For deposition the TEM grids were first cleaned by sonication in pure water for 5 min and then dried and attached to a clean 3-in. microscope slide using a dilute solution of Formvar in spectrophotometric grade chloroform as a weak adhesive. LB multilayers were deposited onto the grids in the usual manner at a rate of 0.5 mm/min. The grids were carefully detached and dried under vacuum for 2 h prior to insertion into the electron microscope.

The tubules used in this work were formed by first dissolving 0.5 mg of $DC_{8,9}PC$ in 5 mL of an ethanol–water mix (70/30% by

(1) Yager, P.; Schoen, P. *Mol. Cryst. Liq. Cryst.* **1984**, *106*, 371–381.
(2) Yager, P.; Scheon, P.; Davies, C.; Price, R.; Singh, A. *Biophys. J.* **1985**, *48*, 899–906.
(3) Georger, J.; Singh, A.; Price, R; Schnur, J.; Yager, P.; Scheon, P. *J. Am. Chem. Soc.* **1987**, *109*, 6169–6175.
(4) Lando, J.; Hansen, J.; Sudiwala, R.; Rickert, S. *Polym. Adv. Technol.* **1990**, *1*, 27–32.
(5) Lando, J.; Hansen, J. *Thin Solid Films* **1989**, *180*, 141–152.
(6) Gaines, Jr., G. L. *Insoluble Monolayers At The Liquid-Gas Interface*; Interscience: New York, 1966.
(7) Johnson, D.; Sanghera, S.; Pons, M.; Chapman, D. *Biochim. Biophys. Acta* **1980**, *602*, 57–69.
(8) Singh, A.; Schnur, J. *Synth. Commun.* **1986**, *16*, 847–852.
(9) Shutt, J. Ph.D. Thesis, Case Western Reserve University, 1987.

0897-4756/90/2802-0594$02.50/0

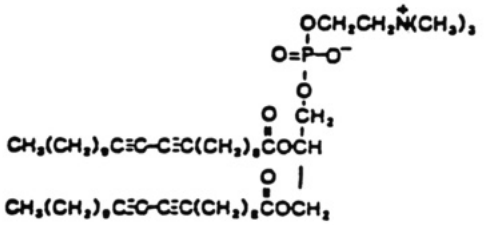

Figure 1. Schematic diagram of $DC_{8,9}PC$ showing atomic labeling system.

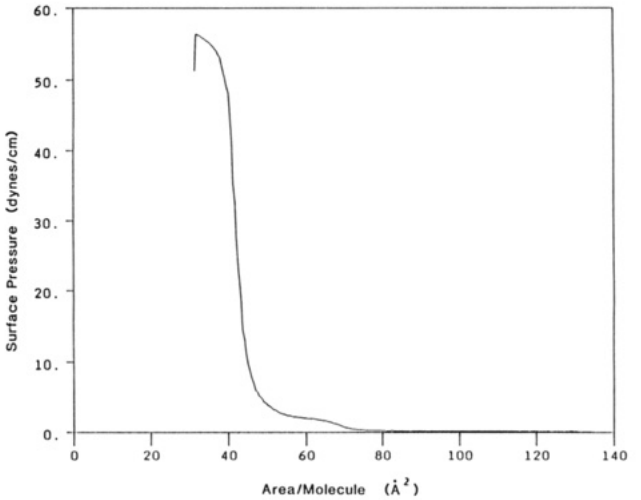

Figure 2. Pressure/area isotherm of $DC_{8,9}PC$ on pure water at 19 °C.

volume ethanol–water) by heating to 60 °C for an hour in a sealed vial. Tubules were then precipitated by allowing the solution to cool slowly to room temperature. It has been shown by Lando et al.[4] that under these conditions tubules are precipitated at 29 °C and have an average diameter and wall thickness of 0.36 and 0.087 μm, respectively. The tubules were then diluted by placing 15 mL of the precipitate into 4 mL of pure water. Samples for diffraction studies were made by placing a drop of this mixture onto a clean carbon-coated TEM grid and drying under vacuum for 4 h before insertion into the electron microscope.

Electron diffraction pictures were recorded at an electron energy of 100 keV on a JEOL JEM-100SX transmission electron microscope operating in the selected area diffraction mode. During the experiment care was taken to reduce sample damage by operating with a very low gun bias voltage, thus keeping the electron dosage to a minimum. The diffraction patterns were persistent for several minutes under these conditions and were recorded photographically with 1–3-min exposure times. No change was noticed in the diffraction patterns that would indicate polymerization of the sample under the electron beam. Reciprocal lattice parameters were measured by comparison to a gold standard photographed under identical conditions. An Optronics System P-100 photoscan digitizer was used to transfer the diffraction pattern to a DEC Microvax II computer allowing accurate integrated intensity measurements to be made. Structural refinement was done using a linked-atom-least-squares (LALS) program developed by Smith and Arnott[10] and atomic electron diffraction scattering factors reported by Grasso.[11]

Results and Discussion

A typical pressure/area isotherm of $DC_{8,9}PC$ on pure water at 19 °C (ambient temperature of the cleanroom) is shown in Figure 2. Film collapse is gradual and begins at about 45 dyn/cm. The Langmuir film showed good stability at surface pressures below 40 dyn/cm. At pressures below about 30 dyn/cm it was found that $DC_{8,9}PC$ deposited on withdrawal of the substrate from the water but came off upon reimmersion. The material was found to deposit reasonable well in a Z-type fashion (i.e., only on withdrawal of the substrate from the water) at a surface pressure of 35 dyn/cm but only if the substrate was initially hydrophilic. Even at this pressure, it was noticed that as the number of layers deposited increased beyond about eight, the deposition ratios progressively decreased and the layers took on a patchy appearance.

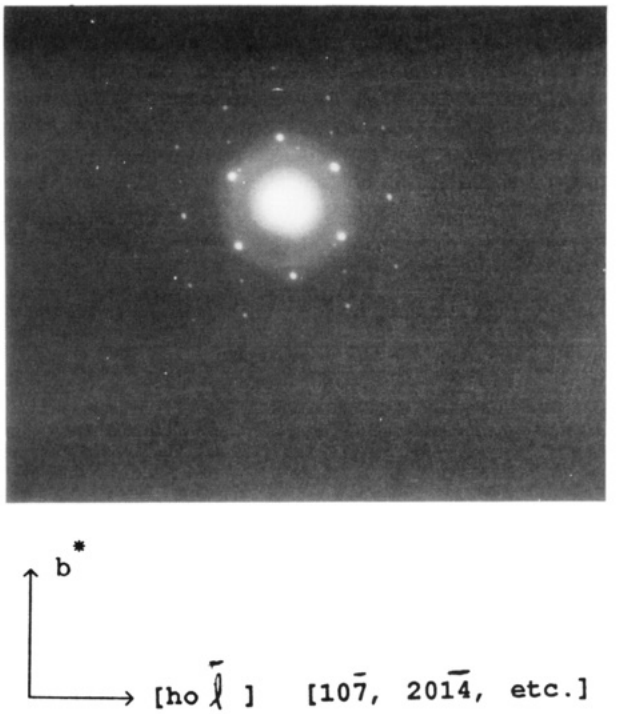

Figure 3. Electron diffraction pattern from a six-layered LB film of $DC_{8,9}PC$. The beam direction is normal to the plane of the film, i.e., along the c^* axis.

The electron diffraction pattern from a six-layered LB film of $DC_{8,9}PC$ is shown in Figure 3. The beam direction is normal to the layer plane. With the analysis outlined in the appendix, the measured unit cell constants are a = 5.90 Å and b = 7.74 Å. These values for a and b, together with the head-to-head, tail-to-tail nature of the layers, suggest two molecules per unit cell. The systematic absences are consistent with a monoclinic system of space group $P2_1$. The b axis is the unique axis.

Twenty-two independent reflections were measured from the pattern in Figure 3, including three systematic absences and two unobserved reflections. These data together with some modeling were used as described in the Appendix to refine the crystal structure of $DC_{8,9}PC$ within LB films. The unit cell density was stepped through the range 1.01–1.25 g/cm^3 (typical of crystalline phospholipids[12–17]). For each density value, the bilayer spacing $c \sin \beta$ was calculated by using eq A3. A structural refinement was then carried out for all reasonable values of c, β, and l as determined from eq A2. First, all the dihedral

(10) Arnott, S.; Campbell Smith, P. S. *Acta. Crystallogr.* **1978**, *A34*, 3–11.
(11) Grasso, R. P.; Lando, J. *J. Mater. Sci. Lett.* **1988**, *7*, 495–496.
(12) Pascher, I.; Sundell, S.; Hauser, H. *J. Mol. Biol.* **1981**, *153*, 791–806.
(13) Pearson, R.; Pascher, I. *Nature* **1979**, *281*, 499–501.
(14) Hitchcock, P.; Mason, R.; Mark Thomas, K.; Graham Shipley, G. *Proc. Natl. Acad. Sci. U.S.A.* **1974**, *71*, 3036–3040.
(15) Elder, M.; Hitchcock, P.; Mason, R.; Shipley, G. *Proc. R. Soc. London, A* **1977**, *354*, 157–170.
(16) Pascher, I.; Sundell, S.; Hauser, H. *J. Mol. Biol.* **1981**, *153*, 807–824.
(17) Suwalsky, M.; Duk, L. *Makromol. Chem.* **1987**, *188*, 599–606.

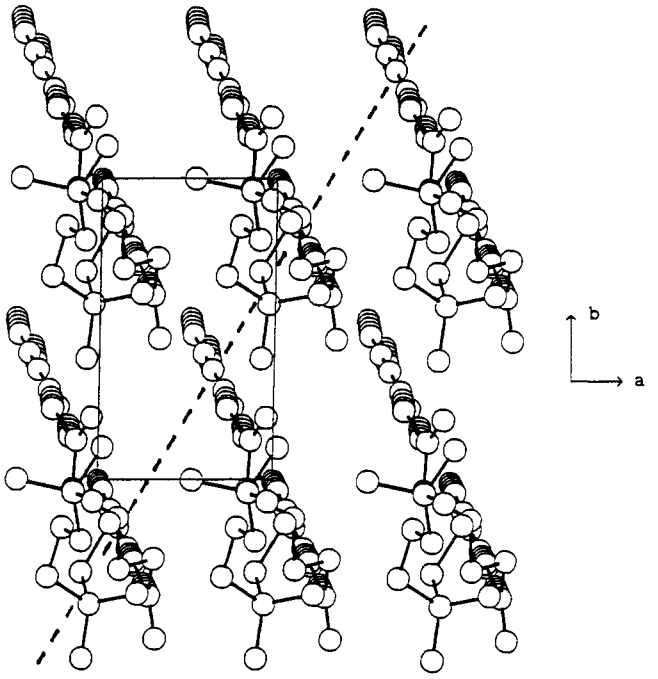

Figure 4. View of the crystal packing of $DC_{8,9}PC$ in LB films looking down the c axis. For clarity the hydrogen atoms have been omitted and only the molecules in the lower half of the unit cell are shown. The dotted line shows the probable direction of polymerization.

Table I. Observed and Calculated Structure Factors of $DC_{8,9}PC$ in LB films (u = Unobserved Reflections, a = Systematic Absences)

refln	F_{obs}	F_{calc}	difference
(1,0,-7)[u]	1.56	2.80	-1.24
(2,0,-14)	15.24	14.83	0.40
(3,0,-21)[u]	1.56	1.64	-0.07
(0,1,0)[a]	0.00	0.00	0.00
(1,1,-7)	20.89	20.25	0.64
(2,1,-14)	5.62	3.97	1.65
(3,1,-21)	7.16	7.09	0.07
(0,2,0)	18.71	18.22	0.49
(1,2,-7)	6.73	7.31	-0.58
(2,2,-14)	9.83	9.58	0.26
(3,2,-21)	4.64	3.22	1.42
(0,3,0)[a]	0.00	0.00	0.00
(1,3,-7)	11.27	11.51	-0.24
(2,3,-14)	6.00	5.93	0.07
(3,3,-21)	2.91	3.19	-0.28
(1,4,-7)	3.88	4.06	-0.19
(2,4,-14)	4.20	2.62	1.58
(3,4,-21)	3.50	1.28	2.22
(0,5,0)[a]	0.00	0.00	0.00
(1,5,-7)	3.87	2.81	1.06
(2,5,-14)	3.18	0.77	2.41
(3,5,-21)	3.18	1.40	1.78

angles listed in Table II and the Eulerean angles for X and Z rotations were refined against contact data. The eight parameters were refined against the diffraction data. These were the scaling and isotropic attenuation factors, the Eulerean angles X and Z, and the four dihedrals α_1, α_3, α_5, and α_6. Refinement of other parameters were considered, but the refinement was most sensitive to those parameters listed above. Because of the high vacuum in the electron microscope, we assumed no water molecules to be present in the structure.

The best structure found was with a unit cell density of 1.1 g/cm^3, which compares favorably with a subsequently measured value of 1.095 g/cm^3 < D < 1.103 g/cm^3 for hydrated tubules.[21] The reflections are indexed as [0,k,0] and [1,k,7], giving c = 78.5 Å and β = 117°. The

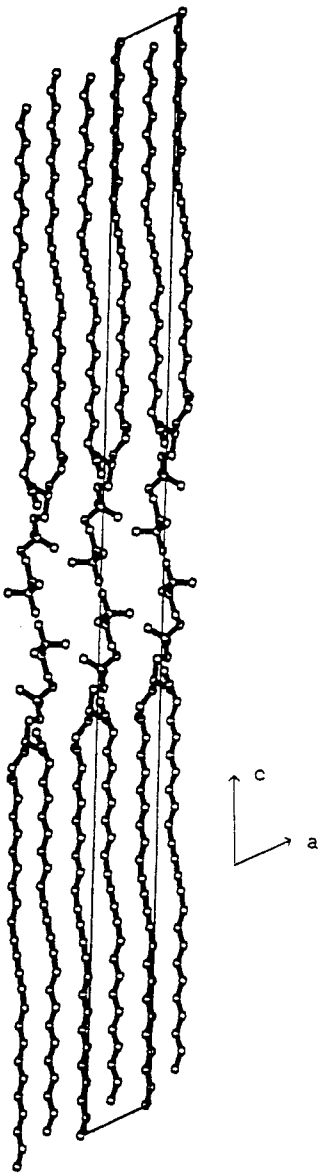

Figure 5. Molecular arrangement of $DC_{8,9}PC$ in LB films looking down the b axis.

Table II. Final Values of the Important Dihedral Angles for $DC_{8,9}PC$ in LB Films (the Naming Scheme Is Shown in Figure 7)

dihedral	angle	dihedral	angle
α_6	-176.9	γ_1	-163.5
α_5	-156.5	γ_2	124.8
α_4	-97.1	γ_3	158.0
α_3	-83.4	β_1	88.4
α_2	86.0	β_2	73.5
α_1	150.5	β_3	145.4
ϑ_1	-28.6	β_4	-37.9
ϑ_3	-151.8	β_5	-174.7

structure is shown in Figures 4–6 and has a weighted residual R = 17.52, where

$$R = 100\Sigma w(F_{cal} - F_{obs})^2/\Sigma w F_{obs}^2$$

Here F_{obs} and F_{cal} are the observed and calculated structure factors, respectively, and w is the weight applied to that reflection. The isotropic attenuation factor is 9.9 Å.[2] Table I lists the measured and calculated structure factors. Table II lists the final values of the important dihedral angles using the naming scheme shown in Figure 7. The remaining dihedral and bond angles are standard theoretical values. Hydrogen atoms are symmetrically placed. Other

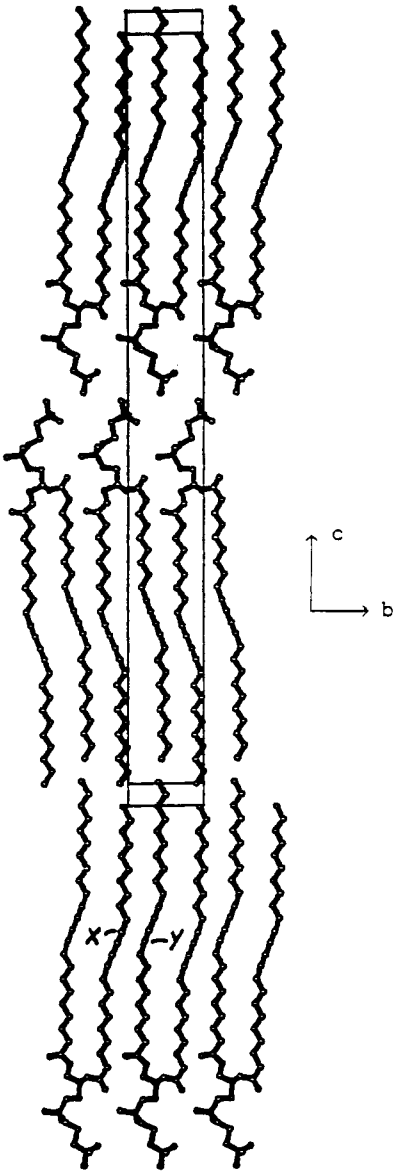

Figure 6. Molecular arrangement of $DC_{8,9}PC$ in LB films looking down the a^* axis.

structures were found with similar or lower residuals but were rejected on the grounds of having too many short contacts or unreasonable values for the attenuation factor. Note also that the 5.09-Å axis was also tried as the unique axis; however, the neccessary tilt required inevitably results in severe short contacts.

Although the residual is reasonably good at 17.52, the headgroup packing shown in Figures 4–6 is not precise. Indeed, a few short contacts exist in the structure shown, but we believe these can be resolved without a major change given more diffraction data. It is also possible that the material is not completely dehydrated as assumed. However, attempts to include a molecule of water within the headgroup resulted in no significant change in residual.

A common feature usually found in crystalline phospholipids is an orthorhombic subcell packing of the hydrocarbon chains.[12,14,15] The diacetylene units seem to determine the chain packing in LB layers of $DC_{8,9}PC$ (Figure 4) and prevent the adoption of the standard orthorhombic subcell. The mode of packing found would appear to facilitate polymerization. It is known that the polymerization of diacetylenes proceeds via a 1,4-addition reaction[18] and is probable if the distance between the reacting carbon atoms is less than 4 Å. The distance between carbon atoms X on the molecule at position (0,0,0) and Y on the molecule at position (0,1,0) (see Figure 6) is 3.78 Å. Polymerization is therefore expected to occur along the direction shown in Figure 4 and would probably involve only a small rotation of the molecules about the c axis. It is reasonable to expect a similar situation to occur in the case of tubules in view of the similarity in lattice spacings (see below). It should be noted that the distance in the monolayer structure of 4.63 Å between molecules along the $d110$ diagonal is somewhat shorter than the ideal diacetylene repeat.

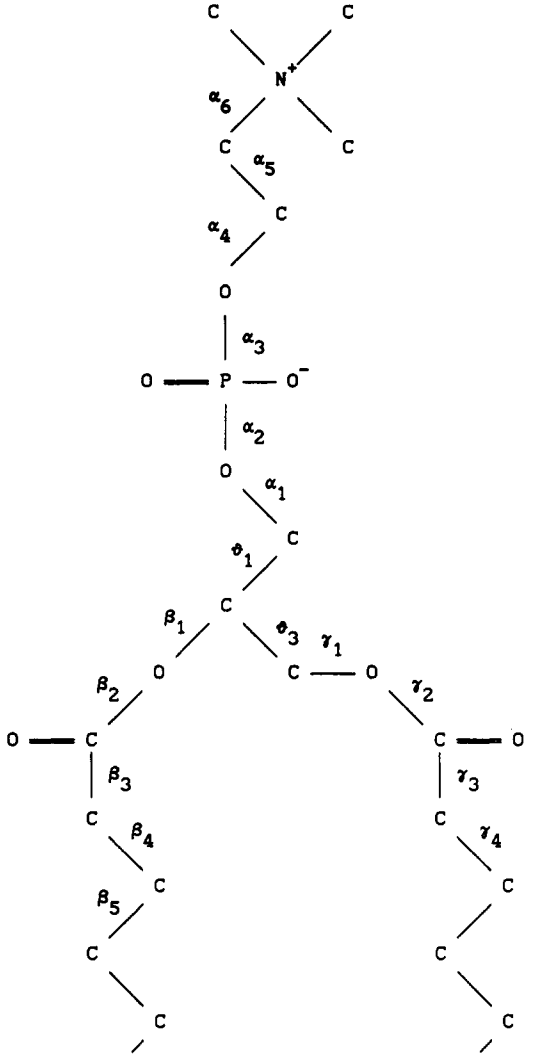

Figure 7. Diagram of the headgroup region of $DC_{8,9}PC$ showing the naming scheme of the dihedral angles listed in Table II.

An electron diffraction pattern of a tubule is shown in Figure 8. The electron beam is incident normal to the tubule walls as shown in Figure 9a. The crystal system is monoclinic as with LB films but with a = 5.18 Å and b = 7.79 Å (unique axis). The structure has not yet been refined as in the case of the LB films, so c and β are not known. The space group is $P2_1$.

An interesting feature of the diffraction pattern from tubules is the doubling of the reflection spots. This is because the incident electron beam is diffracted once by the upper tubule wall and then again by the lower wall; see Figure 9a. If the crystal axes a, b make an angle Δ with respect to the tubule axis, Z, in the upper wall (see Figure

(18) *Polydiacetylenes*; Bloor, D., Chance, R. R., Eds.; Martinus Nijhoff Publishers: Dordrecht, 1985, pp 1–24.

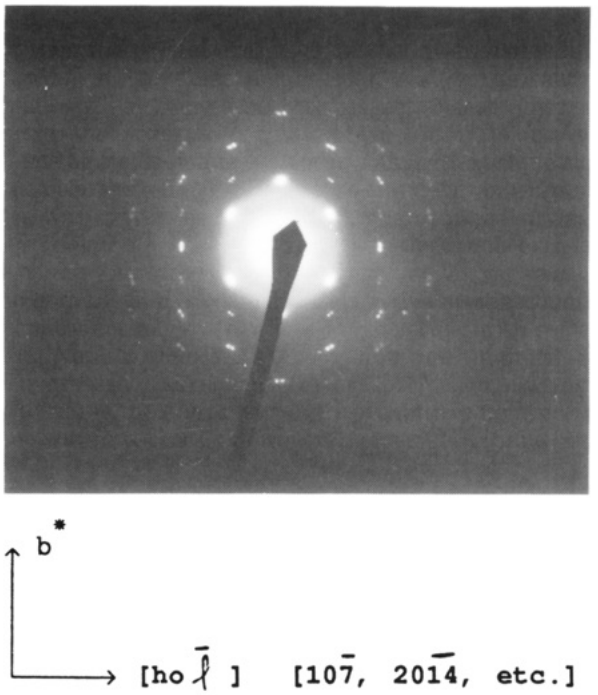

Figure 8. Electron diffraction pattern from a tubule. The beam direction is normal to the tubule wall, i.e., along the c^* axis (see also Figure 9).

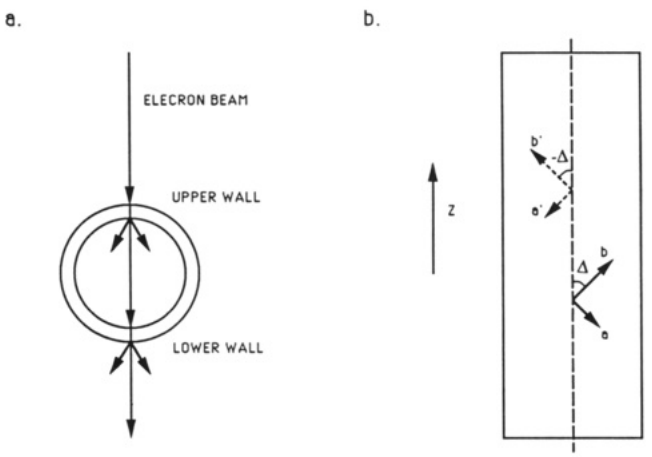

Figure 9. (a) End–on view of a tubule showing the electron beam geometry. The beam is diffracted from both the upper and lower walls. (b) Orientation of the crystallographic axis in the upper (a, b) and lower (a', b') walls with respect to the tubule axis Z.

9b), then the crystal axes a', b' in the lower wall will be at an angle $-\Delta$. This means that the two diffraction patterns will be rotated 2Δ with respect to each other. In practice the patterns are rotated by about 4°. Thus, Δ = 2° and the b axis points very nearly along the tubule axis. If the polymerization direction is as found within LB films, then, within tubules, the polymer chains make an angle $\sin^{-1}(a/b) + \Delta = 43.5°$ with respect to the tubule axis, i.e., the chains follow the helix direction. The bilayer spacing, $c \sin \beta$, in LB films of $DC_{8,9}PC$ is 69.5 Å. This is accounted for almost entirely by the tilt of the molecules with respect to the plane normal, with only a slight interdigitation of the hydrocarbon side chains (Figure 5). Although we have yet to refine the crystal structure, we anticipate a similar value within tubules. However, Schoen et al.[19] and Rhodes[22] report a bilayer spacing in hydrated unpolymerized tubules of 64.7 Å. They suggest a combination of tilt and/or chain interdigitation to account for this. Packing studies suggest that a bilayer spacing as short as 64.7 Å cannot be accommodated with the a and b values that we have found. First, there is insufficient space for the amount of chain interdigidtation required. Second, if the hydrocarbon chain packing is similar to that found in the LB layers, then a further increase in molecular tilt would result in severe short contacts between the chains. Although studies suggest that such a short bilayer spacing may be accommodated by restricting the tilt to about 115° and allowing interdigitation of the headgroup, it is perhaps more likely that there is a difference between fully hydrated and fully dehydrated tubules. Rhodes[22] has noticed that although the bilayer spacing steadily decreases from 65.7 Å as the degree of hydration is lowered, there is phase change below 50% relative humidity. Rhodes does not report the precise nature of the phase change but agrees[23] that an increase in bilayer spacing is possible. We hope to examine these possibilities as part of our program.

Conclusions

Using a combination of electron diffraction techniques and modeling, we have attempted to find the conformation and crystal packing of $DC_{8,9}PC$ within LB layers and tubules. Although the sparsity of data means that the structures presented here can only be approximate, we hope to continue our investigations. In particular, we hope to be able to measure the bilayer spacing in LB films and tubules directly using shadowing techniques and to be able to do a complete refinement of the crystal structure $DC_{8,9}PC$ within tubules. It will be interesting to see how the structures reported here, based to a large extent on modeling, are favored as more diffraction data becomes available. The information gained from the structures will help our understanding of the mechanisms involved in tubule formation.

Appendix

The tilt angle, β, in a monoclinic system means that in general a diffraction pattern cannot be indexed as the a^*b^*net when the beam is incident along the c^* axis. The indexing will depend on c and β. By considering the Ewald sphere constrution for a $[h,0,l]$ reflection and simple trigonometry, it is easy to show that

$$a = dh \tag{A1}$$

$$c \sin \beta = ld \tan \beta^* \tag{A2}$$

where $1/d$ is the magnitude of the scattering vector. This is because the radius of the Ewald sphere, $1/\lambda$, for electrons of energy 100 KeV (λ = 0.037 Å) is very large compared to a^*, b^*, and c^*. We note further that the unit cell density, D_c, for a monoclinic system with Z identical molecules per unit cell is given by

$$D_c = \frac{ZM_W}{0.6021abc \sin \beta} \tag{A3}$$

where M_W is the molecular weight and a, b, and c are in anstroms. The measured value d = 5.09 Å for the lowest order $[h,0,l]$ reflection suggests that $h - l$, and therefore a = 5.09 Å from eq A1. By estimating the unit cell density,

(19) Schoen, P.; Yager, P.; Shreidan, J.; Price, R.; Schnir, J.; Singh, A.; Rhodes, D.; Blechner, S. *Mol. Cryst. Liq. Cryst.* **1987**, *153*, 357–336.
(20) Helfrich, W. *J. Chem. Phys.* **1986**, *85*, 1085–1087.
(21) Lu, M.; Rosenblatt, C., to be published.
(22) Rhodes, D. G.; Blechner, S. L.; Yager, P.; Scheon, P. E. *Chem. Phys. Lipids* **1988**, *49*, 39–47.
(23) Rhodes, D. G., private communication.

one can estimate $c \sin \beta^*$ using eq A3. One can then calculate the values of β^*, and thus c, for different possible l values using eq A2. We have attempted to elucidate the crystal structure by first refining against contact constraints alone so as to minimize contacts between the side chains and from there to refine the headgroup packing using the electron diffraction data. This was done for all reasonable values of D_c, c, β^*, and l.

Registry No. $DC_{8,9}PC$, 109150-63-2.

Formation of Graphite Flakes from Aromatic Precursors: A Comparison of Benzene- and Triphenylene-Derived Graphites

Dong Pyo Kim and M. M. Labes*

Department of Chemistry, Temple University, Philadelphia, Pennsylvania 19122

Received April 4, 1990

The formation of graphite flakes from the decomposition of the aromatic precursors benzene and triphenylene is studied in detail. X-ray diffraction, Raman spectroscopy, scanning electron microscopy, and conductivity measurements are reported as a function of heat treatment temperatures. Benzene appears to form an ideal size nucleus, leading to high-quality oriented graphite, whereas triphenylene-derived graphites are more disordered and undergo exfoliation in the high-temperature annealing process.

Introduction

Carbons that are, at least in part, sp^2 hybridized can be produced in discrete morphological forms by thermal decomposition of precursor fibers or films in a controlled manner. Primary examples of these processes are the preparation of carbon fibers by the decomposition of poly(acrylonitrile) (PAN)[1] or the decomposition of pitch fibers that have been extruded from the mesophase into fiber form.[2,3] Films of PAN[4] and other polymers[5,6] can also be decomposed to give coherent thin films of partially graphitized carbon on an appropriate substrate.

Vapor-phase decomposition of hydrocarbons can also be controlled to give discrete morphological entities under appropriate nucleation conditions. The vapor growth of short carbon fibers (essentially whiskers, VGCF) is based on the observations of the nucleation of carbon whisker growth on fine metal particles. A brief review by Tibbetts of the status of vapor-grown carbon fibers (VGCF) has recently appeared.[7] Koyama and Endo[8] patented a process for producing carbon filaments and fibers by having fine metal particles mix with a hydrocarbon gas near the inlet of a furnace. These filaments consist of nested, rolled-up basal planes of graphite, with a hollow core.[9] Tibbetts[7] proposes a model in which carbon atoms diffuse through the bulk of the metal catalytic particle and precipitate in a graphitic layer growing from the surface of the catalytic particle. These layers are then thickened by vapor-phase deposition of carbon on the exterior surface. Although there is promise to this method, it has not been developed beyond the small-batch noncontinuous fiber production stage. Nevertheless, VGCF fibers have superior thermal and electrical conductivity as compared to PAN-based fibers and are about equal to pitch-based fibers in these properties.

Several vapor decomposition pathways to films have been reported,[10,11] such as the decomposition of 3,4,9,10-perylenetetracarboxylic dianhydride (PTCDA), conducted at 700–900 °C in vacuum.[12] The thickness of the resultant poly(perinaphthalene) (PPN) films varied from several hundred angstroms to approximately 1 μm. Formation of PPN fibers and ribbonlike PPN has also been reported by several groups.[13,14]

In our recent work,[15] we have found conditions under which simple aromatic hydrocarbons and heterocycles can be efficiently converted to highly conducting flakes in a practical and inexpensive manner. Although there is extensive literature dealing with preparation of carbons from such precursors, the morphological characteristics—well-formed flakes—observed in this work are atypical. The approach involves the pyrolysis of hydrocarbon at 800 °C in the presence of halogen vapor. These flakes have a metallic luster and high electrical conductivity and are chemically inert and thermally stable. The starting materials are simple and inexpensive, and the yields of gra-

(1) Donnet, J. B.; Bansal, R. C. *Comprehensive Polymer Science*; Pergamon Press: Oxford, 1989; Vol. 7, p 501.
(2) Lewis, I. C.; Singer, L. S. *Adv. Chem. Ser.* **1988**, 217, 269.
(3) Daumit, G. P. *Carbon* **1989**, *27*, 759.
(4) Renschler, C. L.; Sylwester, A. P.; Salgado, L. V. *J. Mater. Res.* **1989**, *4*, 452.
(5) Ohnishi, T.; Murase, I.; Noguchi, K. *Synth. Met.* **1986**, *14*, 207.
(6) Murakami, M.; Yoshimura, S. *Synth. Met.* **1987**, *18*, 509.
(7) Tibbetts, G. G. *Carbon* **1989**, *27*, 745.
(8) Koyama, T.; Endo, M. Japanese Patent No. 58966, 1982.
(9) Tibbetts, G. G.; Endo, M.; Beetz, C. P. *SAMPE J.* **1986**, *22*, 30.
(10) Fitzer, E.; Mueller, K. *Chemistry and Physics of Carbon*; Marcel Dekker: New York, 1971; Vol. 7, p 237.
(11) Chiang, L. Y.; Stokes, J. P.; Johnston, D.C.; Goshorn, D. P. *Synth. Met.* **1989**, *29*, E483.
(12) Kaplan, M. L.; Schmidt, P. H.; Chen, C.; Walsh, W. M. *Appl. Phys. Lett.* **1980**, *36*, 867.
(13) Iqbal, A.; Ivory, D. M.; Marti, J.; Baughman, R. H. *Mol. Cryst. Liq. Cryst.* **1985**, *118*, 103.
(14) Murakami, M. *Synth. Met.* **1987**, *18*, 531.
(15) Chang, P. H.; Labes, M. M. *Chem. Mater.* **1989**, *1*, 523.

0897-4756/90/2802-0599$02.50/0